Agromet 37 (2): 108-116, 2023

Agromet
journal.ipb.ac.id/index.php/agromet
ISSN : 0126 - 3633

Analysis of Carbon Dioxide Emission from Forest Fires based on Fire Radiative Power in Riau

Mochamad Afif Derma Kusuma, Fithriya Yulisiasih Rohmawati, Idung Risdiyanto
Department of Geophysics and Meteorology, Faculty of Mathematics and Natural Sciences, IPB University, Dramaga Campus, Bogor, Indonesia 16680

ARTICLE INFO

Received
8 March 2023

Revised
12 July 2023

Accepted for Publication
21 August 2023

Published
15 November 2023

doi: 10.29244/j.agromet.37.2.108-116

Correspondence:
Fithriya Yulisiasih Rohmawati
Department of Geophysics and Meteorology, IPB University, Indonesia
Email: fithriyayr@apps.ipb.ac.id

ABSTRACT

Riau is one of the susceptible regions in Indonesia, which faces frequent land and forest fires. Fires occur in various land covers and soil types, both peat and mineral soils, which emitted huge carbon to the atmosphere. Forest fires emit greenhouse gases, including carbon dioxide (CO_2). The objective of the research was to quantify CO_2 from land and forest fires. The quantification emission was for 2016 – 2018 based on the fire radiant power (FRP) dataset along with the buffer methodology for assessing fire-affected land extents across different land covers. The FRP dataset we used to be only at a confidence level of 70% or higher, which represents hotspots. The results revealed large numbers of FRP focal points (> 1000) that can be identified as fires for 2016 and 2018, whereas only small numbers (121) were identified for 2017. Then we quantified the area burned of 95,396 Ha in Riau for 2016, which was double to the 2018's area burned. Further, this burning contributed to CO_2 emission equal to 313,456 tCO_2 for 2016. Emission in 2017 was a relatively low as not many observed fires detected.

KEYWORDS
burned area, emissions, hotspot, land cover, soil types

INTRODUCTION

One of the worst land and forest fires in Indonesia was recorded in Riau Province for 1997/98. When fires occur, carbon was released into the atmosphere in the form of carbon dioxide, carbon monoxide, hydro-carbons, and other kind of sources. Carbon dioxide (CO_2) contributes to 90% of the carbon emissions from land and forest fires events (Jones et al., 2023). CO_2 is a crucial variable in climate change occurrences given the significant surge in the atmosphere over the past decades (Dong et al., 2019). The IPCC asserted that carbon dioxide was the foremost contributor to greenhouse gases, leading to an anthropogenically driven increase in global radiative forcing (IPCC, 2004). Biomass burning plays an important role in the increased concentration of carbon dioxide emissions from Indonesia. The area of forest and land fires as the source of carbon emissions was proportional to the deforestation rate (Adrianto et al., 2019). The carbon emissions have a detrimental impact to environment and human being. Exposure to increased CO_2 leads to several physiological and emotional responses (Duarte et al., 2020). In the long-run, carbon emission induced climate change is largely irreversible (Solomon et al., 2009).

Biomass burning can be detected based on energy radiated during the combustion. The Fire Radiative Power (FRP) is widely applied to measure the radiation from biomass burning (Wooster et al., 2005). This FRP is associated with the intensity of the fire throughout the fire burning process (Laurent et al., 2019). FRP is a good indicator for biomass burning (Engel et al., 2022) compared to the hotspots indicator, which largely depends on high temperature from the surrounding area. Fire radiative power is essentially part of chemical energy liberated from burning vegetation and emitted radiation combustion (Wooster et al., 2005).

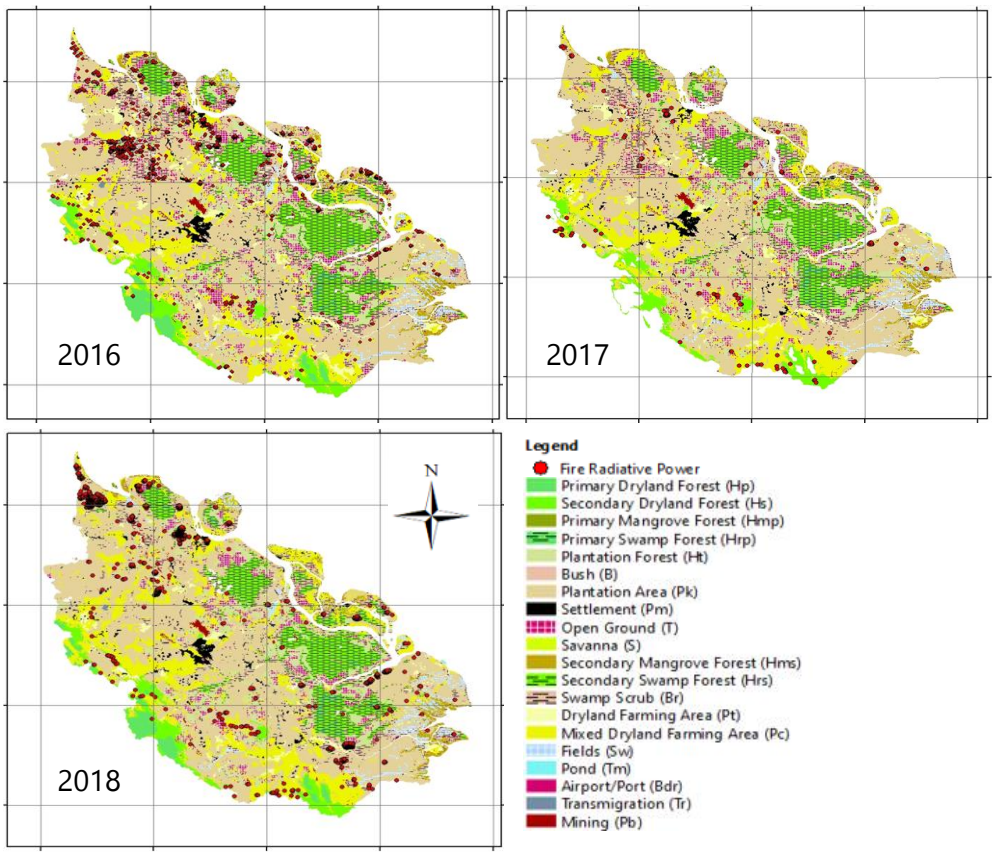

Figure 1. FRP points distribution in Riau Province for 2016-2018.

FRP values provide information on fire dynamics and emissions, particularly in area with frequent fires (da Costa and da Fonseca, 2017). FRP is used to characterize fire types and areas, predict fire hazards, and investigate the interactions between biomass burning, land-cover dynamics, and the hydrological cycle (Li et al., 2018). FRP is taken from the beam on the 4 µm band of the satellite sensor and represents instantaneous radiant energy by an actively burning fire.

Notably, peatland fires present a more intricate challenge in terms of containment due to their capability to propagate not only through aboveground biomass but also penetrate subsurface peat layers (Lisnawati et al., 2022). Riau province has obtained a special awareness as frequent fires occurred especially from peatland ecosystem (Taufik et al., 2023), although restoration efforts were initiated since 2016. The 2015 peat fires contributed to huge carbon emission and potentially influenced human health (Kiely et al., 2019). Therefore, this study aims to quantify CO_2 emissions from Fire Radiative Power (FRP) data in Riau Province.

RESEARCH METHODS

Study Area

Riau Province is categorized into three groups based on it's physical characteristics, including topography, climate, and land cover. The eastern part of Riau is dominated by lowlands with an elevation ranging from 0 to 10 m.a.s.l. The accumulation of organic material in clogged areas in the eastern region leads to the development of peatlands. The accumulation of organic material in clogged areas in the eastern region, which resulted from the slow decomposition of plant matter due to waterlogging, contributes to the formation of peatlands.

Approximately 50% of the land in Riau is covered by peatlands (Pertiwi et al., 2022). Based on the Köppen climate classification, Riau has an Af climate type, while according to the Schmidt and Ferguson the climate type is in the A-B-C range. Based on rainfall patterns, the rainy season usually occurs in the period of October - April and is characterized by high rainfall. The dry season generally occurs in May - September and was characterized by low rainfall (Nurdiati et al., 2022).

Tools and Data Source

The tools used to support this research were among others: (i) ArcGIS 10.5 software to generate a spatial map of FRP distribution in Riau Province; and (ii) Microsoft Excel to process data of the area burned and CO_2 emissions. The fire data was from FIRMS NASA (https://firms2.modaps.eosdis.nasa.gov) at monthly resolution. We used land cover data from Ministry of Environment and Forestry for 2016-2018, whereas soil types distribution data from Global Forest Watch (https://data.globalforestwatch.org/).

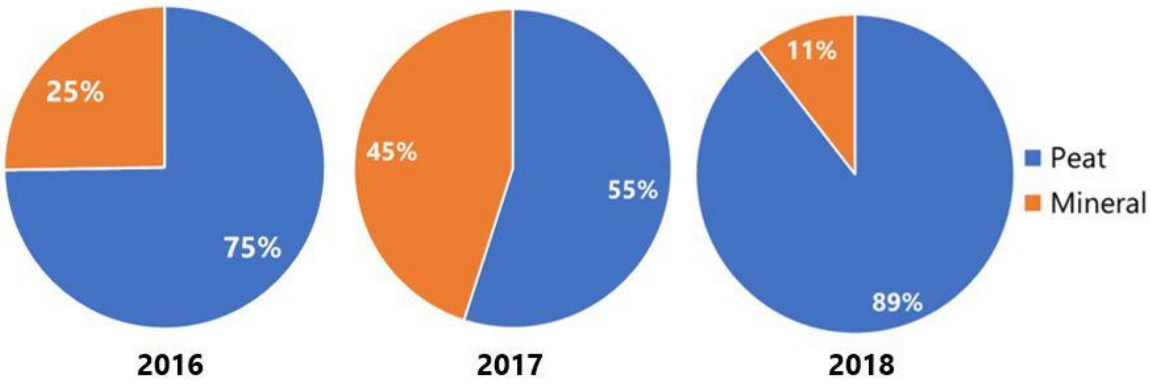

Figure 2. Percentage of estimated total area burned in Riau Province.

Data Processing

Data processing started from land cover data clipped in ArcGIS with the Riau Province area. Subsequently, the data were overlaid with Fire Radiative Power (FRP). FRP distribution data with confidence levels greater than or equal to 70% were used in this study. A high level of confidence implies that it was a hotspot (Hajela et al., 2020; Adiningsih et al., 2006). Then, buffer analysis was performed to estimate the burned area. The area was categorized into peat and mineral burned in the attribute table of ArcGIS.

Estimation of Burned Area

The value of the burned area was obtained from the buffer analysis in ArcGIS. The algorithmic formula used for buffer creation was expressed as F_{buffer} (D, r) (Shen et al., 2018) showed in Equation 1.

$$\beta = F_{buffer}(D, r) \quad (1)$$

where β is single buffer zone pool, D is buffer object, r is buffer radius in km. The output of the buffer analysis was an attribute table with an area of buffer polygon shape. Subsequently, the burned area was calculated within the attribute table based on the results of calculating the polygon area in hectare.

Estimation of Carbon Dioxide Emission

Carbon dioxide emission estimate was calculated using Equation 2 (Seiler and Crutzen, 1980). Variables B and E were adjusted for each land cover type, as shows in Table A1. After the mass value of the fuel was determined, further calculations were performed to calculate the carbon biomass. In tropical forests, carbon accounts for 45% of forest mass (Saharjo et al., 2015) (Equation 3).

$$M = A \times B \times E \quad (2)$$

$$M(C) = 0.45 \times M \quad (3)$$

where M is mass of burned fuel (tons), A is area of burned area (ha), B is fuel load (ton/ha), E is burning efficiency.

The next step was to calculate carbon dioxide emissions. CO_2 emissions were calculated using two formulas for peat and mineral soils. Carbon dioxide emissions from peat soils were calculated using Equation 4. In peatland fires, approximately 50% of the peat mass was in the form of carbon. During the burning period in peat soils, approximately 77% of the combustion output was CO_2. To compute the carbon dioxide emissions from mineral soils, Equation 5 was employed. The estimation of carbon dioxide emissions within mineral soils stood out due to the fact that in instances of fires transpiring within tropical forests, approximately 90% of the resultant combustion products constituted CO_2 gas (Saharjo et al., 2015).

$$M(CO_2) = 0.5 \times 0.7 \times M(C) \quad (4)$$

$$M(CO_2) = 0.9 \times M(C) \quad (5)$$

where M(C) is carbon biomass (tons), and $M(CO_2)$ is carbon dioxide emission (tons).

Land Cover

The Riau Province's land cover in 2016, 2017, and 2018 consisted of 21 types, with a total area of 8,882,800 Ha (Table A1). The primary forest area decreased annually from 154,400 Ha in 2016 to 149,900 Ha in 2018. The area of secondary forests also decreased by 5% within two years. Along with the reduction in forest land cover area, the area of plantations and mixed dryland agriculture is increasing annually, with the largest area of 3,541,200 Ha in 2018. From 2016 to 2017, the total area of primary and secondary dry forests decreased by 13,000 Ha from 469,200 Ha to 456,200 Ha. The plantation area increased from 3,084,300 Ha in 2016 to 3,305,300 Ha in 2017. Mixed dryland agricultural increased from 1,281,800 Ha in 2016 to 1,356,900 Ha in 2017.

Alterations within this region transpired between 2017 and 2018. Roughly 6,400 Ha of primary and secondary forest zones experienced a reduction, declining from 456,200 Ha to 449,800 Ha. territory dedicated to mixed dryland agriculture escalated from

Figure 3. Estimation of burned area on various land covers in Riau Province for 2016, 2017, 2018.

1,356,900 Ha to 1,535,400 Ha. The increased in plantation area occurred due to social and economic reasons for the local population (Rangga et al., 2020). Forest and land fires were among the most influential major causes of land use change in Indonesia (Adrianto et al., 2019; Alisjahbana and Busch, 2017).

RESULTS AND DISCUSSION

Land Cover Changes

Plantation areas and swamp shrub had a greater cumulative amount of FRP for each year (Figure 1). For example, in 2018 the plantation area was the place where the most FRP points were 723 points consisting of 682 points on peat soils and 40 points on mineral soils. In 2017, the plantation area was the most area with 53 FRP points, consisting of 47 points on peat soils and 6 points on mineral soils. In 2016, the swamp shrub area was the area that had the most FRP points, namely 507 points, consisting of 432 points on peat soils and 75 points on mineral soils.

In mixed dryland agriculture, the distribution of Fire Radiative Power (FRP) appeared to be more widespread compared to other land cover types (Figure 1). This distribution of FRP points had a significant impact on the estimation of the extent of burned areas, which tended to be more extensive. It was suspected that the distribution of FRP points was primarily attributed to activities such as land clearing for plantations, agricultural practices, plantation forestry, and transmigration.

Consequently, the quantity and spatial distribution of FRP points exert a notable influence on the calculation of burned area and carbon dioxide emissions (Cruz-Lopez et al., 2019). Specifically, land cover types characterized by a lower number of FRP points resulted in smaller burned areas and consequently emit lower amounts of carbon dioxide in comparison to land cover types with a higher density of FRP points (Fisher et al., 2020). Moreover, the number of FRP points detected also varies according to the type of underlying soil, distinguishing between peat and mineral soil categories.

Peat soil was the area with the most fires because it is flammable and contains a lot of organic matter from the remains of plants and other organic matter (Graham et al., 2022; Hayasaka et al., 2020). Page and Hooijer (2016) mentioned that peat fires in Southeast Asia could last for days, weeks, or even months and are exceedingly difficult to control. The rainfall affected the number of FRP points. The number of FRP points increased when the rainfall intensity was low, and vice versa. Rainfall affected the fluctuation of hotspots in a region (Kumar and Kumar, 2022; Richardson et al., 2022). Seasons also played a role in determining the number of FRP points. The number of FRP points in the dry season was relatively greater than in the rainy season. From three-year period, the average number of FRP points detected during the dry season was 724, while in the rainy season, it was 282. Kumar and Kumar (2022); Abram et al., (2021) stated that the smaller the rainfall intensity, the greater the number of fires, and vice versa.

Burned Area Estimation

The calculation for estimating the burned area uses FRP points with a confidence level greater than or equal to 70%. This confidence level indicated that there

Table 1. Estimation of carbon dioxide emissions of mineral soils and peatlands in 2016, 2017 and 2018.

Year	CO_2 emission on mineral lands (ton)	CO_2 emission on peat lands (ton)	Total (ton)
2016	147,561	165,896	313,457
2017	24,110	10,826	34,936
2018	37,602	117,859	155,461

was fire in the area (Pinto et al., 2020). Therefore, the calculation of the fire burned area by the Ministry of Environment and Forestry was used as a comparison of the results of this study. The estimated burned area in 2016 was 95,396 ha. The incidence of fires in peatland areas was 71,293 ha (75%) (Figure 1).

The most extensively burned area based on land cover was in the swamp shrub area (Br) of 33,778 Ha (Figure 3). In addition to swamp shrub, open space (T) and plantations (Pk) were burned more than in other areas. The area of open land burned was 21,851 Ha, or approximately 23% of the total area burned, where the area of peatland was the most burned, namely 28,785 ha, while minerals only 4,993 Ha. The area of plantations burned was 20,982 Ha, or about 22% of the total burned area, which consisted of fires on peatlands covering an area of 17,318 Ha and mineral soils covering 3,664 Ha.

The estimated area burned in 2017 was 6,911 Ha. The incidence of fires in the peatland areas was 3,800 Ha (55%) (Figure 2). The plantation area (Pk) had the largest burned area at 3,052 Ha (Figure 3). Plantation land on peatlands with a burnt area of 2,706 ha and minerals of 346 Ha. The area burned in the mixed dryland agriculture (Pc) in 2017 differed from that in other years. The area with the largest burned area was mineral soil, with an area of 1,324 Ha, while there was no burned area for peat soil. The results showed no burned area in peat soil because no FRP points were detected in the mixed dryland agriculture. This also occurred in secondary dryland forest (Hs) areas, where the burned area was only on mineral soils. Fires on plantations were more prevalent in peatlands and estimated to be caused by peatland drainage practices in plantations (Taufik et al., 2019).

The estimated area burned in 2018 was 46,545 Ha. The most widespread fires occurred in peatland areas of 41,565 Ha (89%) (Figure 1). The plantation area (Pk) was the largest burned compared to other land cover types in 2018. 27,164 Ha of plantations were burned, with peat soil as the largest burned area at 25,661 Ha and mineral soil at 1,503 Ha. In addition to plantation areas, mixed dryland agriculture (Pc) area fires were also wider than other land covers, namely 7,742 Ha, consisting of 6,199 Ha in peat soils and 1,542 Ha in mineral soils (Figure 3).

Carbon Dioxide Emission

Carbon dioxide emissions were from the fuel mass using the fuel load and burning efficiency of various land covers (Table A1). In 2016, land and forest fires emitted the largest amount of CO_2 in range 2016-2018 (Table 1). In mineral soils, the largest emissions were produced from swamp shrub (Br) and plantation (Pk) land covers of 30,331 tCO_2 and 29,676 tCO_2 (Figure A1), respectively. In peat soils, swamp shrub emitted 68,004 tCO_2. The lowest CO_2 emissions of 402 tCO_2 were emitted from dryland agricultural areas (Pt). Swamp shrub (Br) areas were land cover vulnerable to fire hazards because they contain many light fuels (Stavi, 2019). In 2017, the lowest CO_2 emissions occurred within the 2016-2018 period, with mineral soils and peat soils contributing 24,110 tCO_2 and 10,826 tCO_2, respectively, for a combined total of 34,936 tCO_2.

These results were consistent with research by Saharjo and Putri (2019) conducted in Ketapang district, when yearly 2017 had the lowest CO_2 estimate, related to the low number of hotspots. In peat soils, the plantation area had the highest CO_2 emissions (8,523 tCO_2), while the open ground area (T) had the lowest CO_2 emissions at 145 tCO_2 (Figure A1). In 2018, it emitted 155,461 tCO_2 of carbon dioxide, with mineral soils of 37,602 tCO_2 and peat soils of 117,859 tCO_2. One of the causes of forest and land fires is access land, such as plantation development (Gaveau et al., 2019). In estimating carbon dioxide emissions, the greater the emission figure, the more vegetation will burn (Saranya et al., 2016).

CONCLUSIONS

The determination of the extent of the fire-affected area can be achieved through the application of a buffering method, wherein the distribution of FRP (Fire Radiative Power) points was expanded with a confidence interval exceeding 70%. The respective quantities of CO_2 emissions for the fire incidents in the years 2016, 2017, and 2018 were 313,456 tCO_2, 34,963 tCO_2, and 155,460 tCO_2. Notably, fires occurred in peatlands in the years 2016 and 2018 resulted in notably higher CO_2 emissions compared to those on mineral soils. In 2016, forest and land fires predominantly encompassed swamp shrub situated

on peat soils spanning 28,785 Ha, alongside open land areas on mineral soils covering 5,859 Ha. The peatland fires of 2017 were primarily characterized by plantations, accounting for 2,706 Ha, while mineral soils were dominated by mixed dryland agriculture, encompassing 1,324 Ha. Similar patterns were observed in 2018, with peat soils predominantly affected by fires in plantations spanning 25,661 Ha, and mineral soils predominantly impacted by mixed dryland agriculture, covering 1,542 Ha.

ACKNOWLEDGEMENT

The authors thank to the anonymous reviewers and editor for their insightful comments and constructive suggestions, which significantly enhanced the quality of this manuscript.

REFERENCES

Abram, N.J., Henley, B.J., Sen Gupta, A., Lippmann, T.J.R., Clarke, H., Dowdy, A.J., Sharples, J.J., Nolan, R.H., Zhang, T., Wooster, M.J., Wurtzel, J.B., Meissner, K.J., Pitman, A.J., Ukkola, A.M., Murphy, B.P., Tapper, N.J., Boer, M.M., 2021. Connections of climate change and variability to large and extreme forest fires in southeast Australia. Communications Earth & Environment 2, 8. https://doi.org/10.1038/s43247-020-00065-8.

Adiningsih, E.S, Tejasukmana, B.S, Khomarudin, M.R., 2006. Dynamical land/forest fire hazard mapping of Kalimantan based on spatial and satellite data. Agromet 20, 1-9. https://doi.org/10.29244/j.agromet.20.1.1-9.

Adrianto, H.A., Spracklen, D.V., Arnold, S.R., Sitanggang, I.S., Syaufina, L., 2020. Forest and Land Fires Are Mainly Associated with Deforestation in Riau Province, Indonesia. Remote Sensing 12, 3. https://doi.org/10.3390/rs12010003.

Alisjahbana, A.S., Busch, J.M., 2017. Forestry, Forest Fires, and Climate Change in Indonesia. Bulletin of Indonesian Economic Studies 53, 111–136. https://doi.org/10.1080/00074918.2017.1365404.

Cruz-Lopez, M.I., Manzo-Delgado, L., Aguirre-Gómez, R., Chuvieco, E., Equihua-Benítez, J.A., 2019. Spatial Distribution of Forest Fire Emissions: A Case Study in Three Mexican Ecoregions. Remote Sensing 11, 1185. https://doi.org/10.3390/rs11101185.

da Costa, B.S.C., da Fonseca, E.L., 2017. The use of Fire Radiative Power to estimate the biomass consumption coefficient for temperate grasslands in the Atlantic Forest Biome. Revista Brasileira de Meteorologia 32, 255-260. http://dx.doi.org/1-0.1590/0102-77863220004.

Dong, K., Dong, X., Dong, C., 2019. Determinants of the global and regional CO2 emissions: What causes what and where?. Applied Economics, 1-14. https://doi.org/10.1080/00036846.2019.1606410.

Duarte, C.M., Jaremko, L., Jaremko, M., 2020. Hypothesis: Potentially systemic impacts of elevated CO_2 on the human proteome and health. Frontiers in Public Health 8, 1-9. https://doi.org/10.3389/fpubh.2020.543322.

Engel, C.B., Jones, S.D., Reinke, K.J., 2022. Fire Radiative Power (FRP) values for biogeographical region and individual geostationary HHMMSS Threshold (BRIGHT) hotspot derived from the Advanced Himawari Imager (AHI). Remote Sensing 14, 2540. https://doi.org/10.3390/rs14112540.

Fisher, D., Wooster, M.J., Xu, W., Thomas, G., Lestari, P., 2020. Top-down estimation of particulate matter emissions from extreme tropical peatland fires using geostationary satellite fire radiative power observations. Sensor 20, 7075. https://doi.org/10.3390%2Fs20247075.

Gaveau, D.L.A., Epting, J., Lyne, O., Linkie, M., Kumara, I., Kanninen, M., Leader-Williams, N., 2009. Evaluating whether protected areas reduce tropical deforestation in Sumatra. Journal of Biogeography 36, 2165-2175. https://doi.org/10.1111/j.1365- 699.2009.02147.x.

Gaveau, D.L.A., Locatelli, B., Salim, M.A., Yaen, H., Pacheco, P., Sheil, D., 2019. Rise and fall of forest loss and industrial plantations in Borneo (2000–2017). Conservation Letters 12, e12622. https://doi.org/10.1111/conl.12622.

Graham, L.L.B., Applegate, G.B., Thomas, A., Ryan, K.C., Saharjo, B.H., Cochrane, M.A., 2022. A Field Study of Tropical Peat Fire Behaviour and Associated Carbon Emissions. Fire 5, 62. https://doi.org/10.33 90/fire5030062.

Hajela, G., Chawla, M., Rasool, A., 2020. A Clustering Based Hotspot Identification Approach For Crime Prediction. Procedia Computer Science 167, 1462–1470. https://doi.org/10.1016/j.procs.2020.03.357.

Hayasaka, H., Usup, A., Naito, D., 2020. New Approach Evaluating Peatland Fires in Indonesian Factors. Remote Sensing 12. https://doi.org/10.3390/rs12122055.

IPCC, 2004. Capturing carbon dioxide directly from the atmosphere. World Resource Review 16,157-172.

Jones, M.W., Peters, G.P., Gasser, T., 2023. National contributions to climate change due to historical emissions of carbon dioxide, methane, and nitrous oxide since 1850. Scientific Data 10, 155. https://doi.org/10.1038/s41597-023-02041-1.

Kiely, L., Spracklen, D.V., Wiedinmyer, C., Conibear, L.,

Reddington, C.L., Archer-Nicholls, S., Lowe, D., Arnold, S.R., Knote, C., Khan, M.F., Latif, M.T., Kuwata, M., Budisulistiorini, S.H., Syaufina, L., 2019. New estimate of particulate emissions from Indonesian peat fires in 2015. Atmospheric Chemistry and Physics 19, 11105–11121. https://doi.org/10.5194/acp-19-11105-2019.

Kumar, S., Kumar, A., 2022. Hotspot and trend analysis of forest fires and its relation to climatic factors in the western Himalayas. Natural Hazards 114, 3529–3544. https://doi.org/10.1007/s11069-022-05530-5.

Laurent, P., Mouillot, F., Moreno, M.V., Yue, C. and Ciais, P., 2019. Varying relationships between fire radiative power and fire size at a global scale. Biogeosciences 16, 275-288. https://doi.org/ 10.5194/bg-16-275-2019.

Li, F., Zhang, X., Kondragunta, S., Csiszar, I., 2018. Comparison of fire radiative power estimates from VIIRS and MODIS observations. Journal of Geophysical Research: Atmospheres 123, 4545-4563. https://doi.org/10.1029/2017JD 027823.

Lisnawati, Taufik, M., Dasanto, B.D., Sopaheluwakan, A., 2022. Fire Danger on Jambi Peatland Indonesia based on Weather Research and Forecasting Model. Agromet 36, 1–10. https://doi.org/10.29244/j.agromet.36.1.1-10.

Nurdiati, S., Sopaheluwakan, A., Septiawan, P., Ardhana, M.R., 2022. Joint Spatio-Temporal Analysis of Various Wildfire and Drought Indicators in Indonesia. Atmosphere 13. https://doi.org /10.3390/atmos13101591.

Page S.E., Hooijer, A., 2016. In the line of fire: the peatlands of Southeast Asia. Philosophical Transactions of the Royal Society: Biological Sciences 371, 1-9. https://doi.org/10.1098/rstb.2015.0176.

Pertiwi, N., Tsusaka, T.W., Nguyen, T.P.L., Abe, I., Sasaki, N., 2022. Nature-based Carbon Pricing of Full Ecosystem Services for Peatland Conservation-A Case Study in Riau Province, Indonesia. Nature-Based Solutions 2, 100023. https://doi.org /10.1016/j.nbsj.2022.100023.

Pinto, M.M., DaCamara, C.C., Hurduc, A., Trigo, R.M., Trigo, I.F., 2020. Enhancing the fire weather index with atmospheric instability information. Environmental Research Letters 15, 0940b7. https://doi.org/10.1088/1748-9326/ab9e22.

Rangga, K.K., Yonariza, Yanfika, H., Mutolib, A., 2020. Perception, attitude, and motive of local community towards forest conversion to plantation in Dharmasraya District, West Sumatra, Indonesia. Biodiversitas Journal of Biological Diversity 21, 10-17. https://doi.org/10.13057/biodiv/d211057.

Richardson, D., Black, A.S., Irving, D., Matear, R.J., Monselesan, D.P., Risbey, J.S., Squire, D.T., Tozer, C.R., 2022. Global increase in wildfire potential from compound fire weather and drought. npj Climate and Atmospheric Science 5, 23. https://doi.org/10.1038/s41612-022-00248-4.

Saharjo, B.H., Putra, E.I., Syam, N., 2015. Carbondioxide (CO_2) Emission Estimation Caused by Forest Fires on Different Land Covers in South Sumatra Province in 2000-2009. Jurnal Silvikultur Tropika. 6,132-138. https://doi.org/10.29244/j-siltrop.

Saranya, K.R.L., Reddy, C.S., Rao, P.V.V.P., 2016. Estimating carbon emissions from forest fires over a decade in Similipal Biosphere Reserve, India. Remote Sensing Applications: Society and Environment 4. https://doi.org/10.1016/j.rsase.2016.06.001.

Seiler, W., Crutzen, P.J., 1980. Estimates of gross and net fluxes of carbon between the biosphere and the atmosphere from biomass burning. Climatic Change 2, 207–247. https://doi.org/10.1007/BF00137988.

Shen, J., Chen, L., Wu, Y., Jing, N., 2018. Approach to Accelerating Dissolved Vector Buffer Generation in Distributed In-Memory Cluster Architecture. ISPRS International Journal of Geo-Information 7. https://doi.org/10.3390/ijgi7010026.

Solomon, S., Plattner, G.K., Knutti, R., Friedlingstein, P., 2009. Irreversible climate change due to carbon dioxide emissions. Proceedings of the National Academy of Sciences 106, 1704–1709. https://doi.org/10.1073/pnas.0812721106.

Stavi, I., 2019. Wildfires in Grasslands and Shrublands: A Review of Impacts on Vegetation, Soil, Hydrology, and Geomorphology. Water 11. https://doi.org/10.3390/w11051042.

Taufik, M., Setiawan, B.I., Van Lanen, H.A.J., 2019. Increased fire hazard in human-modified wetlands in Southeast Asia. Ambio 48, 363–373. https://doi.org/10.1007/s13280-018-1082-3.

Taufik, M., Haikal, M., Widyastuti, M.T., Arif, C., Santikayasa, I.P., 2023. The Impact of Rewetting Peatland on Fire Hazard in Riau, Indonesia. Sustainability 15. https://doi.org/10.3390/su15032169.

Wooster, M.J., Roberts, G., Perry, G.L.W., Kaufman, Y.J., 2005. Retrieval of biomass combustion rates and totals from fire radiative power observations: FRP derivation and calibration relationships between biomass consumption and fire radiative energy release. Journal of Geophysical Research: Atmospheres 110. https://doi.org/10.1029/2005JD006318.

ANNEX

Table A1. Fuel Load, Burning Efficiency Coefficient, and Land Cover area of Riau Province in 2016-2018.

No	Type of Land Cover	Fuel Load (ton/ha)	Burning Efficiency	Land Cover (thousand ha)		
				2016	2017	2018
1	Primary dryland forest (Hp)	70	0.4	154.4	150	149.9
2	Secondary dryland forest (Hs)	50	0.5	314.8	306.2	299.9
3	Primary swamp forest (Hrp)	70	0.4	51.9	51.7	50.8
4	Secondary swamp forest (Hrs)	50	0.4	973.4	944.1	934.6
5	Primary mangrove forest (Hmp)	-	-	4.9	3.1	3.1
6	Secondary mangrove forest (Hms)	30	0.5	164.3	168.8	167.9
7	Plantation forest (Ht)	50	0.5	954	680.3	654.3
8	Shrub (B)	25	0.8	39.2	33.4	34
9	Swamp shrub (Br)	30	0.5	859	755.5	606.9
10	Savanna (S)	-	-	0.1	0	0
11	Plantation (Pk)	40	0.5	3,084.3	3,305.3	3,541.2
12	Dryland farming (Pt)	30	0.7	246.7	185.1	154.4
13	Mixed dryland agriculture (Pc)	20	0.7	1,281.8	1,356.9	1,535.4
14	Transmigration (Tr)	-	-	3.9	3.9	3.9
15	Rice fields (Sw)	10	0.9	159.6	166.4	166.1
16	Pond (Tm)	-	-	2.2	2.5	2.5
17	Open space (T)	10	0.8	382.2	558	361.5
18	Mining (Pb)	5	0.8	36.1	38.3	38.7
19	Settlement (Pm)	5	0.8	143.4	146	147.4
20	Swamp (Rw)	-	-	25.9	26.3	29.5
21	Airport/Harbour (Bdr)	-	-	0.8	0.9	0.9
Total				**8,882.8**	**8,882.8**	**8,882.8**

Figure A1. Estimation of carbon dioxide (CO_2) emissions each year in mineral lands (left panel) and peat land (right panel) Riau Province.